Interannual variability of summertime aerosol optical depth over East Asia during 2000–2011: a potential influence from El Niño Southern Oscillation

To cite this article: Yikun Liu *et al* 2013 *Environ. Res. Lett.* **8** 044034

View the article online for updates and enhancements.

Related content

- Environmental effects of the recent emission changes in China: implications for particulate matter pollution and soil acidification
  Bin Zhao, Shuxiao Wang, Xinyi Dong et al.

- Impacts of the East Asian monsoon on lower tropospheric ozone over coastal South China
  Derong Zhou, Aijun Ding, Huiting Mao et al.

- Multiscale periodicities in aerosol optical depth over India
  S Ramachandran, Sayantan Ghosh, Amit Verma et al.

Recent citations

- Impact of 2015–2016El Niño and 2017–2018 La Niña on PM2.5 concentrations across China
  Xiaohong Wang *et al*

- Dissimilar effects of two El Niño types on PM2.5 concentrations in East Asia
  Jaein I. Jeong *et al*

- Variations of Haze Pollution in China Modulated by Thermal Forcing of the Western Pacific Warm Pool
  Yingchang You *et al*

Interannual variability of summertime aerosol optical depth over East Asia during 2000–2011: a potential influence from El Niño Southern Oscillation

Yikun Liu[1,2,3]**, Junfeng Liu**[1,4] **and Shu Tao**[1]

[1] College of Urban and Environmental Sciences, Peking University, Beijing, People's Republic of China
[2] College of Physics, Peking University, Beijing, People's Republic of China

E-mail: jfliu@pku.edu.cn

Abstract

Aerosols degrade air quality, perturb atmospheric radiation, and impact regional and global climate. Due to the rapid increase in anthropogenic emissions, aerosol loading over East Asia (EA) is markedly higher than other industrialized regions, which motivates a need to characterize the evolution of aerosols and understand the associated drivers. Based on the MISR satellite data during 2000–2011, a wave-like interannual variation of summertime aerosol optical depth (SAOD) is observed over the highly populated North China Plain (NCP) in East Asia. Specifically, the peak-to-trough ratio of SAOD ranges from 1.4 to 1.6, with a period of 3–4 years. This variation pattern differs apparently from what has been seen in EA emissions, indicating a periodic change in regional climate pattern during the past decade.

Investigations of meteorological fields over the region reveal that the high SAOD is generally associated with the enhanced Philippine Sea Anticyclone Anomaly (PSAA) which weakens southeasterlies over northeastern EA and depresses air ventilation. Alternatively, higher temperature and lower relative humidity are found to be coincident with reduced SAOD. The behavior of PSAA has been found previously to be modulated by the El Niño Southern Oscillations (ENSO), therefore ENSO could disturb the EA SAOD as well. Rather than changing coherently with the ENSO activity, the SAOD peaks over NCP are found to be accompanied by the rapid transition of El Niño warm to cold phases developed four months ahead. An index measuring the development of ENSO during January–April is able to capture the interannual variability of SAOD over NCP during 2000–2011. This finding indicates a need to integrate the large-scale periodic climate variability in the design of regional air quality policy.

Keywords: inter-annual variability, AOD, El Niño, East Asia, ENSO, air quality

S Online supplementary data available from stacks.iop.org/ERL/8/044034/mmedia

[3] Present address: Department of Earth and Environmental Science, College of Liberal and Professional Studies, University of Pennsylvania, PA, USA.
[4] Address for correspondence: College of Urban and Environmental Sciences, Peking University, Beijing, 100871, People's Republic of China.

1. Introduction

Ambient aerosols adversely impact human health (Janssen *et al* 2011, Pope *et al* 2002, Liu *et al* 2009a), reduce visibility (Park *et al* 2003, Langridge *et al* 2012) and perturb climate (Kaufman *et al* 2002, Ramanathan *et al* 2001). These negative

effects raise a need to better constrain the factors which control the abundance of aerosols and its evolution from regional to global scale.

Aerosols originate from direct release of primary emissions or indirect formation through oxidation of precursor gases (e.g., SO_2 and VOCs, Liu *et al* 2009b). Large variability in aerosol concentrations may have significant consequences on regional climate and human health. Both scattering (e.g., sulfate, nitrate, and organics) and absorbing (e.g., dust, black and brown carbon) aerosols change atmospheric radiation, leading to a cooling/warming effect on global climate (Koch *et al* 2011). Besides, hydrophobic (e.g., dust, black carbon and part of primary organic matters) and hydrophilic (e.g., sulfate, nitrate, and secondary organics) aerosols initiate ice and liquid clouds (Prenni *et al* 2009, Ming *et al* 2007), and enhance the melting of land snow and sea ice cover (Mahowald *et al* 2011). These effects alter the earth albedo, and perturb global radiation budget. Moreover, particulate matter with aerodynamic diameter less than 2.5 μm (PM2.5) can penetrate deep into the lungs, causing cardiovascular disease, lung cancer, and premature death (Pope *et al* 2002, Liu *et al* 2009a).

In contrast to the long-lived species, such as CO_2 and CH_4, aerosol concentrations vary significantly over space and time, mainly driven by the short lifetime of aerosols (∼1 week) (Liu *et al* 2009b) and the spatiotemporal inhomogeneity of emission sources (Lamarque *et al* 2010, Lin *et al* 2010). The distribution and evolution of global aerosol loading are observed continuously by satellite remote sensing as aerosol optical depth (AOD). The AOD data are widely used to understand the trend of emissions and the variability of air quality (e.g., Kaufman *et al* 2002, Li *et al* 2010, Lin *et al* 2010).

While the trend in anthropogenic emissions plays an important role in shaping the AOD fluctuation, climate perturbations may affect AOD independently of changes in anthropogenic emissions through alterations of meteorological conditions and natural emissions. For instance, surface ozone is strongly correlated with temperature during summertime stagnant conditions (Jacob and Winner 2009). The export of Saharan dust and biomass burnings in tropics is found to be correlated with El Niño Southern Oscillation (ENSO) which is one of the prominent modes of large-scale climate variability (Hsu *et al* 2012).

However, over the populated regions, some researchers have observed a decreasing trend of AOD over the eastern US and Europe and a significant increasing trend of AOD over the eastern China and India (Augustine *et al* 2008, Hsu *et al* 2012), which mainly reflect a change in local anthropogenic emissions (Hsu *et al* 2012). For example in East Asia (EA), the bottom-up anthropogenic emissions have shown that SO_2 emissions (i.e., the precursors of sulfate aerosols) from China are tripled from 1980 to 2010 (peaked in 2006, Smith *et al* 2011). Other pollutants, such as NO_x, black carbon (BC) and organic matter (OM), mostly show an increasing trend during the same period (Wang *et al* 2012). This rapid increase in anthropogenic emissions significantly enhances aerosol loading, and leads to severe air quality problems over China.

This study evaluates the interannual variability of AOD over EA and targets the underlying meteorological and climate drivers that impose on the fluctuation of AOD. Specifically, we focus on addressing the extent that the AOD variability over EA is tied to specific meteorological fields and large-scale climate perturbations like the ENSO. After a brief discussion of the data and method used in this study (section 2), we describe the seasonal and interannual variability of AOD over EA (AOD_{EA}), and examine the potential meteorological drivers based on correlation analysis (section 3). We then extend our exploration to the association of AOD_{EA} to ENSO activities (section 4), and postulate the mechanism to explain this connection (section 5). Finally, we discuss the science and policy implications in section 6.

2. Data and methods

We acquired the multi-angle imaging spectroradiometer (MISR) (Diner *et al* 1998) level 3 AOD products at 558 nm (with horizontal resolution of 0.5° × 0.5°) from the Atmospheric Sciences Data Center at NASA (http://eosweb.larc.nasa.gov). Compared to the ground based observations, MISR retrievals well depict the temporal aerosol trend in China with lowest biases in summer (Liu *et al* 2010). Moreover, MISR data are more suitable than moderate resolution imaging Spectroradiometer (MODIS) retrievals in analyzing long-term and low-frequency variability, particularly over bright backgrounds (e.g., arid and semi-arid regions or large urban centers where high surface reflection and the lack of dense vegetation can bias MODIS retrievals) (Liu *et al* 2009c).

We analyze the MISR seasonal AOD data from 2000 to 2011, with a special focus on AOD above three subregions over the populated East Asia (e.g., the north China plain (NCP), southeastern China (SEC), and southwestern Japan (SWJ)). To evaluate the association of AOD to regional meteorological fields, we acquired the NCEP/NCAR reanalysis monthly data for the surface temperature, surface pressure, zonal and meridional wind, and relative humidity, which are provided by NOAA/OAR/ESRL PSD, Boulder, Colorado, USA (www.esrl.noaa.gov/psd/). In addition, we obtained monthly precipitation data from the Global Precipitation Climatology Project (GPCP, version 2) (Adler *et al* 2003).

To investigate the relationship between El Niño/La Niña events and AOD, we acquired the multivariate ENSO index (Wolter and Timlin 2011) (MEI) from www.esrl.noaa.gov/psd/enso/mei/ and the Niño 3.4 index (Barnston *et al* 1997) from http://climexp.knmi.nl/data/inino5.dat. Wolter and Timlin (2011) pointed out that the MEI index provides a more complete and flexible description of the ENSO phenomenon than single variable ENSO indices such as the Southern Oscillation index (SOI) or the Niño 3.4 index. Therefore, the MEI index is employed in this study to depict the variability of El Niño/La Niña episodes.

The association of interannual variability of AOD to meteorological fields and the ENSO index are examined based
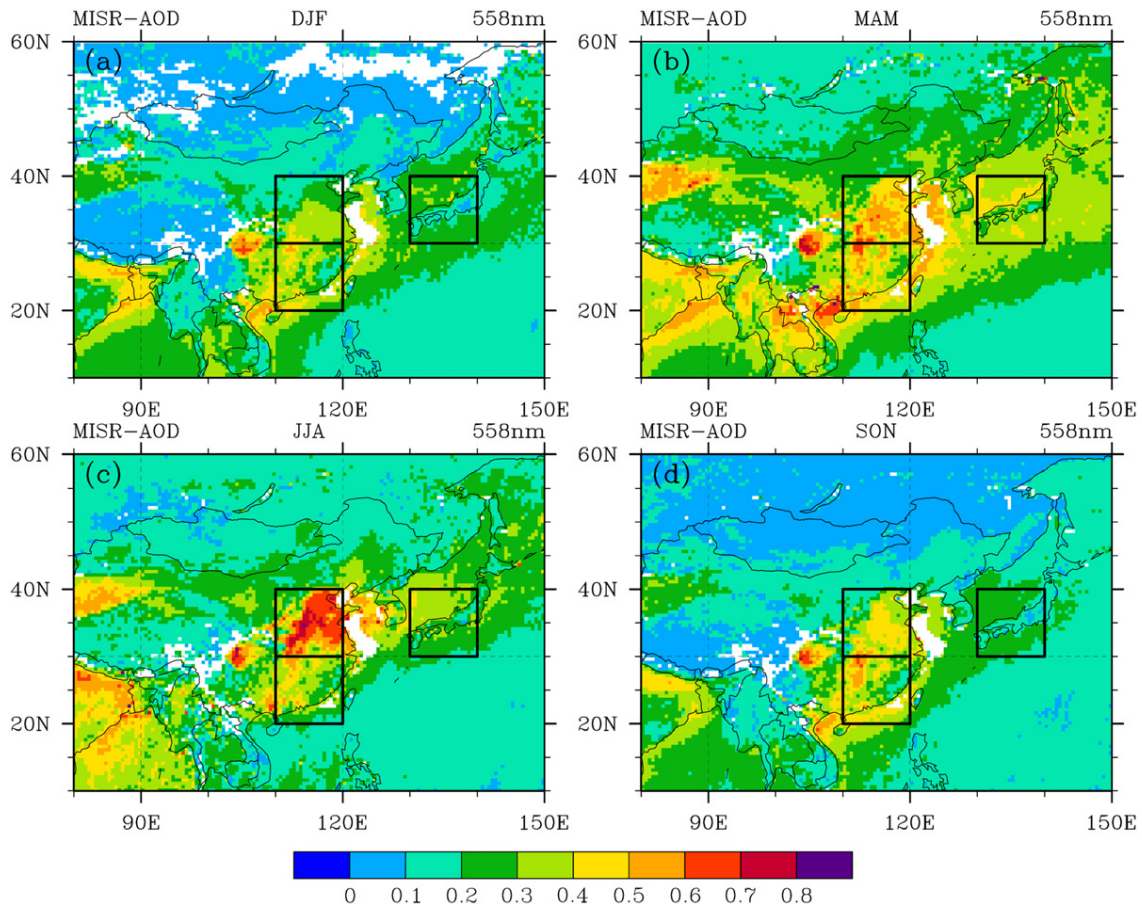
Figure 1. Seasonal averaged MISR AOD (at 558 nm) over EA in (a) December–January–February (DJF), (b) March–April–May (MAM), (c) June–July–August (JJA), and (d) September–October–November (SON) during 2000–2011. The three rectangle regions represent the North China Plain (NCP, upper left), southeastern China (SEC, below), and southwestern Japan (SWJ, upper right).

on correlation analysis. Correlation coefficients between two variables (e.g., X and Y) are calculated as:

$$\text{corr}(X, Y) = \frac{\text{cov}(X, Y)}{\sigma_X \sigma_Y} \qquad (1)$$

where $\text{cov}(X, Y)$ represents the covariance between X and Y. σ_X and σ_Y are standard deviations of X and Y, respectively. Since the MISR archive starts in 2000, AOD data used in this study are limited to a 12-year period. Therefore, correlations less than 0.5 are not significant at the 95% confidence interval (CI).

In order to quantitatively understand the interannual association between AOD_{EA} and the ENSO activity, a linear regression is employed to explore the connection:

$$\text{reg}(X, Y) = \text{corr}(X, Y) \frac{\sigma_Y}{\sigma_X} \qquad (2)$$

where $\text{corr}(X, Y)$ is the correlation coefficient between X and Y. The regression analysis indicates the change of AOD_{EA} as a result of unit change of the ENSO index.

## 3. Seasonal and interannual variability of AOD over EA

As shown in figure 1, East Asia, particularly the NCP, is masked by thick aerosol cloud with seasonal AOD

ranges from less than 0.4 in winter to more than 0.7 in summer. Unlike other regions such as Africa and the Amazon where high aerosol loadings originate from natural sources (i.e., dust or biomass burning), the high AOD over EA (AOD_{EA}) is mainly contributed by anthropogenic emissions of SO_2, BC and organic aerosols (as well as the springtime dust particles transported from the deserts in northwestern China and Mongolia, see figure S1 in the supplementary materials available at stacks.iop.org/ERL/8/044034/mmedia for locations), which enhance ambient loadings of both primary and secondary aerosols (Tao *et al* 2012) and lead to frequent occurrence of severe haze over EA. Reddy *et al* (2005) estimated that sulfate, organic matter, and black carbon, respectively account for 60–80%, 5–10%, and 2–6% of total AOD_{EA}.

The AOD_{EA} exhibits a distinct seasonal variation pattern (figure 1) that the lowest AOD_{EA} appears in December–January–February (DJF, i.e., the boreal winter) and the highest shows in June–July–August (JJA, i.e., the boreal summer). During boreal winter, frequent cold fronts sweep the pollution away and replace it with clean polar air. In addition, formation of secondary aerosols (i.e., sulfate and SOA) becomes slower due to a lack of oxidants and precursor gases (Liu *et al* 2010, He *et al* 2013). In spring, prevailing winds (see figure S2 in the supplementary
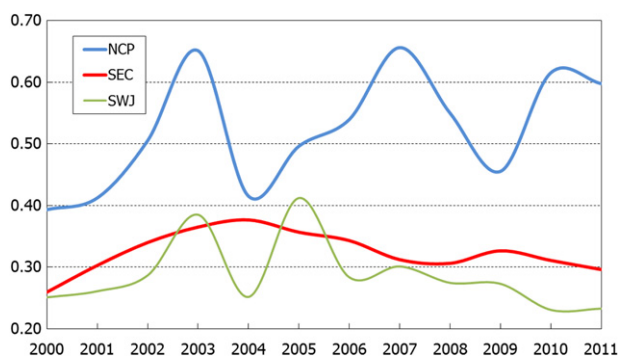
Figure 2. Interannual variability of SAOD averaged over three regions in East Asia. Blue line indicates the NCP (30°–40°N, 110°–120°E), red line indicates the SEC (i.e., 20°–30°N, 110°–120°E), and the yellow line indicates the rectangle region containing the SWJ (i.e., 30°–40°N, 130°–140°E).

materials available at stacks.iop.org/ERL/8/044034/mmedia) carry biomass burning and dust plumes from Southeast Asia and Mongolia to EA (Deng *et al* 2008, Peters *et al* 2009), which coincides with the enhanced local sources and significantly elevates AOD levels over almost entire EA (Liu *et al* 2010).

During the boreal summer, the prevailing East Asian monsoon over southern China dilutes and scavenges air pollutants, resulting in a decreased summertime AOD (SAOD) (Zhu *et al* 2012). In contrast, over northeastern EA particularly the NCP, the SAOD climbs to its maximum for a year due to a number of reasons such as enhanced production of secondary aerosols and increased moisture (Liu *et al* 2010, Fu *et al* 2012, Heald *et al* 2010). After summer, AOD_{EA} falls back to a level analogous to that in spring, but prominent AOD only stands over the eastern China.

Figure 1 depicts a relative maximum of AOD over the NCP in JJA, coincident with the most populated region in China. When averaging the SAOD over the NCP (30°–40°N, 110°–120°E, i.e., $SAOD_{NCP}$), a wave-like interannual variation of the $SAOD_{NCP}$ is observed (figure 2). The $SAOD_{NCP}$ peaks are stable at ∼0.65 with a period of 3–4 years, exceeding the troughs (∼0.45) by 40–60%. Over southeastern China (20°–30°N, 110°–120°E), the fluctuation of SAOD is similar to that in NCP, but with a much weaker amplitude and an opposite phase, probably caused by a north–south shift of East Asian monsoon. Over Japan (45°–55°N, 140°–150°E), the variability of SAOD is different to either NCP or SEC, particularly after 2006.

The changes in local emissions or meteorological patterns could influence aerosols abundance and light extinction, resulting in SAOD fluctuation. As shown in Reddy *et al* (2005), the SAOD over EA is mostly anthropogenic origin. However, the wave-like oscillation of $SAOD_{NCP}$ is seemingly different to either the inverted U-shaped trend (maximum in 2006) of SO_2 emissions (see figure 2 in Lu *et al* 2011) or the mono-increasing trend of BC and OC emissions from China (see figure 5 in Lu *et al* 2011). This difference indicates that during 2000–2011, the change of $SAOD_{NCP}$ might be caused by factors beyond local anthropogenic emissions.

AOD measures the integrated extinction of aerosols on the atmospheric column. Its magnitude is determined by both aerosol column number density and light extinction efficiency. Aerosol types and their mixing states (i.e., internally or externally mixed) determine the refractive index and thereby the extinction efficiency of aerosols. Aerosol column abundance modulates the cumulative extinction of solar radiation. As a result, meteorological factors could influence AOD via either aerosol abundance or its extinction ability. Temperature, wind/pressure, and precipitation could influence the formation, transport and removal of aerosols, which alter aerosols spatiotemporal distribution. Relative humidity (RH) controls the uptake of water vapor by hydrophilic aerosols, directly influencing aerosol extinction efficiency.

To understand the potential effect of changing meteorological fields on the interannual variability of $SAOD_{NCP}$, we conducted a correlation analysis over the East Asian domain. Figure 3 shows the correlation coefficients between $SAOD_{NCP}$ and different meteorological factors (i.e., surface temperature, RH, precipitation and SLP/wind fields) in each reanalysis grid during 2000–2011. As shown in figure 3(a), a weak anti-correlation pattern between $SAOD_{NCP}$ and surface temperature resides over the Yellow Sea, opposed to a weak positive association spreading over the southeastern China. This correlation pattern indicates that a lower temperature to the east of NCP or a higher temperature to the south of NCP may be associated with higher $SAOD_{NCP}$. Correlation alone does not stand for the cause–effect relationship. Therefore, lower temperature could be either the cause of (e.g., lower temperature is usually associated with higher RH, which increases aerosols water uptake and light extinction, and enhances multiphase formation of semi-volatile organic species (Liu *et al* 2012)) or caused by (e.g., sometimes dense fog or scattering aerosols may block sunlight and cool the surface air) higher AOD. Therefore, to understand the mechanism which fundamentally determines the dynamical feedbacks between AOD and surface temperature over NCP, more analysis on the detailed chemical, physical and dynamical processes based on the fully coupled global climate model is needed, and will be examined in the follow-up studies.

Figure 3(b) shows that the relationship between AOD_{NCP} and RH follows a similar pattern to that of surface temperature depicted in figure 3(a) but with a reversed signal. In particular, the RH over the Yellow Sea and south Japan is positively correlated with $SAOD_{NCP}$. Higher RH could enhance the uptake of water for water-soluble aerosols (e.g., sulfate, nitrate and certain organic species) and therefore increase aerosols extinction coefficient. In contrast, precipitation in general is an indicator measuring the removal of aerosols. However, precipitation itself is influenced by the abundance of aerosols. Aerosol particles may act as cloud condensation nuclei (CCN) and ice nuclei (IN), which modify cloud properties (e.g. cloud droplet size and lifetime) and precipitation (e.g., Denman *et al* 2007). As inferred from figure 3(c), there is no direct linkage between precipitation and the fluctuation of $SAOD_{NCP}$ during the past decade.
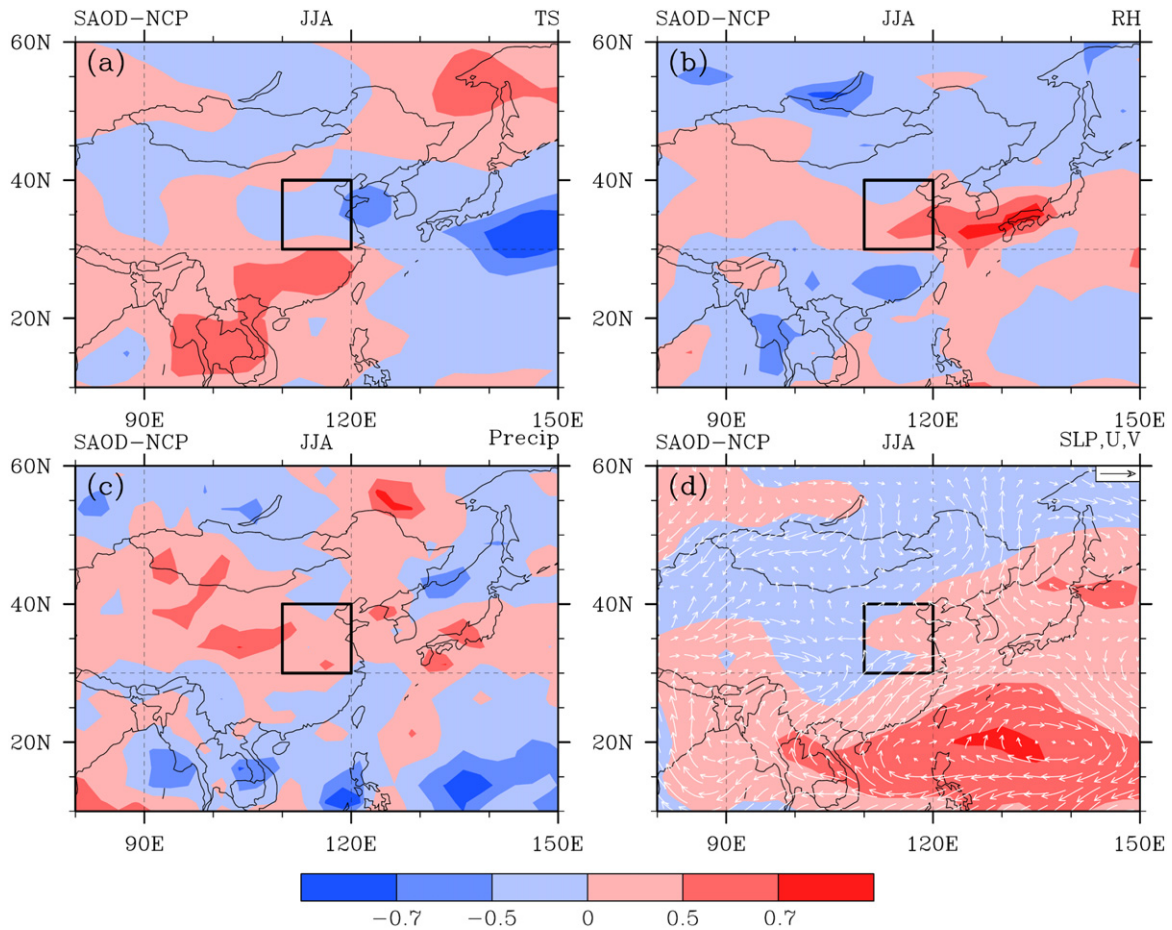
Figure 3. Horizontal distribution of the correlation coefficients between the SAOD$_{NCP}$ and seasonal averaged (a) surface temperature (TS), (b) surface relative humidity (RH), (c) precipitation, and (d) sea level pressure (SLP, colors) and wind fields at 850 hPa (U, V, arrows) at each reanalysis grid during 2000–2011. The black rectangle is NCP.

Figure 3(d) shows the correlations of SAOD$_{NCP}$ to the surface pressure (i.e., colors) and 850 mb wind field (i.e., arrows). SAOD$_{NCP}$ is strongly associated with a large-scale anticyclonic circulation anomaly over the western equatorial Pacific, and positively correlated with surface pressure centered at the Philippine Sea. This correlation indicates that SAOD$_{NCP}$ is linked to atmospheric circulation pattern over the western subtropical Pacific. Figure S2 (available at stacks.iop.org/ERL/8/044034/mmedia) depicts the summer mean surface pressure and wind vectors averaged from 2000 to 2011 over EA. Southeastern China is influenced by the air mass from South China Sea, while the air quality over NCP is mostly influenced by the air mass transported from the Yellow Sea. The intrusion of clean maritime inflows from western Pacific significantly dilutes aerosol pollution and decreases the SAOD$_{NCP}$. Figure 3(d) also reveals that an intensified Philippine Sea subtropical high would trigger an anticyclone anomaly circulated over the eastern EA, which would block eastward transport of clean air from western Pacific and foster stagnation conditions favoring air pollution episodes over NCP. Therefore, the fluctuation of SAOD$_{NCP}$ is associated to the climate variability over western Pacific. Zhu *et al* (2012) simulated the surface PM2.5 concentrations over EA based on the global chemical transport model

GEOS-CHEM driven with the assimilated meteorological fields. By comparing to the change of East Asian summer monsoon index, they indicated that the increases in surface aerosol concentrations over eastern China are contributed by decadal-scale weakening of the East Asian summer monsoon.

4. Potential influence by the El Niño episodes

ENSO is the most prominent coupled atmosphere–ocean phenomenon that causes seasonal and interannual variability of global climate (Wolter and Timlin 2011). ENSO is also believed to impact precipitation over East China (Feng and Hu 2004, Xue and Liu 2008). As indicated by Lau and Nath (2006), many ENSO-related circulation changes in East Asia are connected to the evolution of Philippine Sea anticyclone anomalies (PSAA). Therefore, the linkage of SAOD$_{NCP}$ to PSAA elicits a hypothesis that the variability of SAOD$_{NCP}$ is influenced considerably by the El Niño episodes.
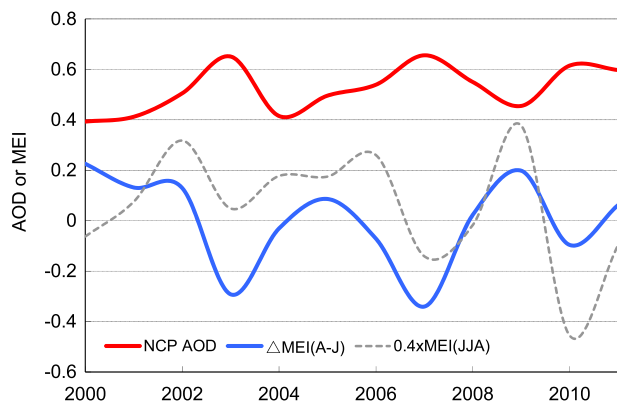
However, the interannual variability of SAOD$_{NCP}$ is not directly linked to the amplitude of ENSO episodes. Figure 4 shows that the variability of SAOD$_{NCP}$ is inconsistent with the time series of multivariable El Niño index (MEI) averaged in JJA. Results are similar for the Niño 3.4 index. As indicated by Wang *et al* (2009), summer monsoon over the South China

Table 1. Pearson correlation coefficients between $SAOD_{NCP}$ and the change of MEI index in different seasons.

	ΔMEI_{F-D}[a]	ΔMEI_{M-M}[a]	ΔMEI_{A-J}[a]	ΔMEI_{N-S}[a]	ΔMEI_{A-J}[a]
$SAOD_{NCP}$	−0.13	−0.60[b]	−0.37	0.12	−0.80[b]

[a] ΔMEI_{F-D} is calculated as $(MEI_{Feb} - MEI_{Dec(previous\ year)})/2$; ΔMEI_{M-M} is $(MEI_{May} - MEI_{Mar})/2$; ΔMEI_{A-J} is $(MEI_{Aug} - MEI_{Jun})/2$; ΔMEI_{N-S} is $(MEI_{Nov} - MEI_{Sep})/2$; ΔMEI_{A-J} is calculated as $(MEI_{Apr} - MEI_{Jan})/3$.
[b] Significant at 95% confidence interval.

Figure 4. Interannual variability (2000–2011) of $SAOD_{NCP}$ (red line), ΔMEI_{A-J} (blue line) and MEI index (dashed line) averaged over JJA (scaled by a factor of 0.4).

Sea is mainly affected by the decaying phase of ENSO after 1970s. The ENSO's influence on summer monsoon infers that rather than the strength of El Niño episodes, the rate of ENSO change could play an important role in affecting $SAOD_{NCP}$ anomalies.

Table 1 lists the correlation coefficients between the $SAOD_{NCP}$ and the rate of change in the MEI index in different seasons. Correlation is highest during the winter–spring season, specifically in a period from January to April (represented as ΔMEI_{A-J}), indicating that a rapid transition from El Niño cold to warm phase during January to April is generally followed by a suppressed $SAOD_{NCP}$ (see the anti-correlation pattern in figure 4). In general, years with lower ΔMEI_{A-J} (here 'lower ΔMEI_{A-J}' means more negative ΔMEI_{A-J} values) are associated with higher $SAOD_{NCP}$, and vice versa. It suggests that the ambient air quality and visibility over the most populated region in EA could be markedly influenced by the sea surface temperature (SST) anomalies over the equatorial eastern Pacific.

5. Mechanism driving the interannual variability of $SAOD_{NCP}$

The role of remote ENSO forcing from the equatorial central Pacific in setting up the subsequent large-scale circulation pattern in controlling the summertime air pollution and AOD loadings over the NCP could be partially explained by the association between the ΔMEI_{A-J} index and development of tropical equatorial Pacific meteorological fields (i.e., the SLP, wind fields and surface temperature) from the boreal winter to summer (figure 5). A positive ΔMEI_{A-J} index in general

depicts a rapid SST increase over the eastern equatorial Pacific during the transition period from winter to spring (see figure S3 in the supplementary materials available at stacks.iop.org/ERL/8/044034/mmedia). During JFM, a positive ΔMEI_{A-J} index is accompanied by an above-normal high pressure anomaly (figure 5 or below-normal low temperature anomaly, figure S3 available at stacks.iop.org/ERL/8/044034/mmedia) over the eastern equatorial Pacific, characterized mainly by a La Niña signal. In spring, a high ΔMEI_{A-J} index is generally subject to the retreat of high pressure anomaly and an enhancement of SST over the equatorial Pacific. This high ΔMEI_{A-J} index potentially generates a heat source which forces a cyclone anomaly over the North Pacific from mid-spring to summer (Lau and Nath 2006). Results from the stationary wave model calculation confirmed such a low pressure anomaly inferred from the meteorological difference between prominent El Niño and La Niña episodes (Lau and Nath 2006). Besides the low pressure anomaly at the mid-latitude Pacific, two more low pressure anomaly centers emerge at the eastern and western equatorial pacific (figures 5(d)–(e)) during years with high ΔMEI_{A-J} index. The one residing over the western subtropical Pacific generates a cyclonic wind vector anomaly at 850 hPa, which intensifies the maritime inflow over the NCP, significantly ameliorating the air quality during high ΔMEI_{A-J} summers.

This ENSO-induced meteorological development feature persists even beyond the period 2000–2011. As shown in figure S4 in the supplementary materials (available at stacks.iop.org/ERL/8/044034/mmedia), a rapid westward displacement of the North Pacific low pressure anomaly from April to August is observed coincident with high ΔMEI_{A-J} during 1980–2011. This coincidence indicates that summertime air quality and radiative forcing over NCP could be inherently modulated by the pace of springtime transition of El Niño cold/warm phases.

6. Discussions

AOD measures the aerosol column extinction which is affected by both emissions and climate perturbations. Quantitatively decomposing the change of $SAOD_{NCP}$ into these two components relies on detailed process analysis in the state-of-the-science climate modeling system as well as accurate estimation of spatiotemporal variability of regional emissions. While the oscillation of $SAOD_{NCP}$ is found to be relevant to the ENSO activities, emission changes, triggered by economic growth/recession, urbanization, and implementation of emission control regulations (not fully
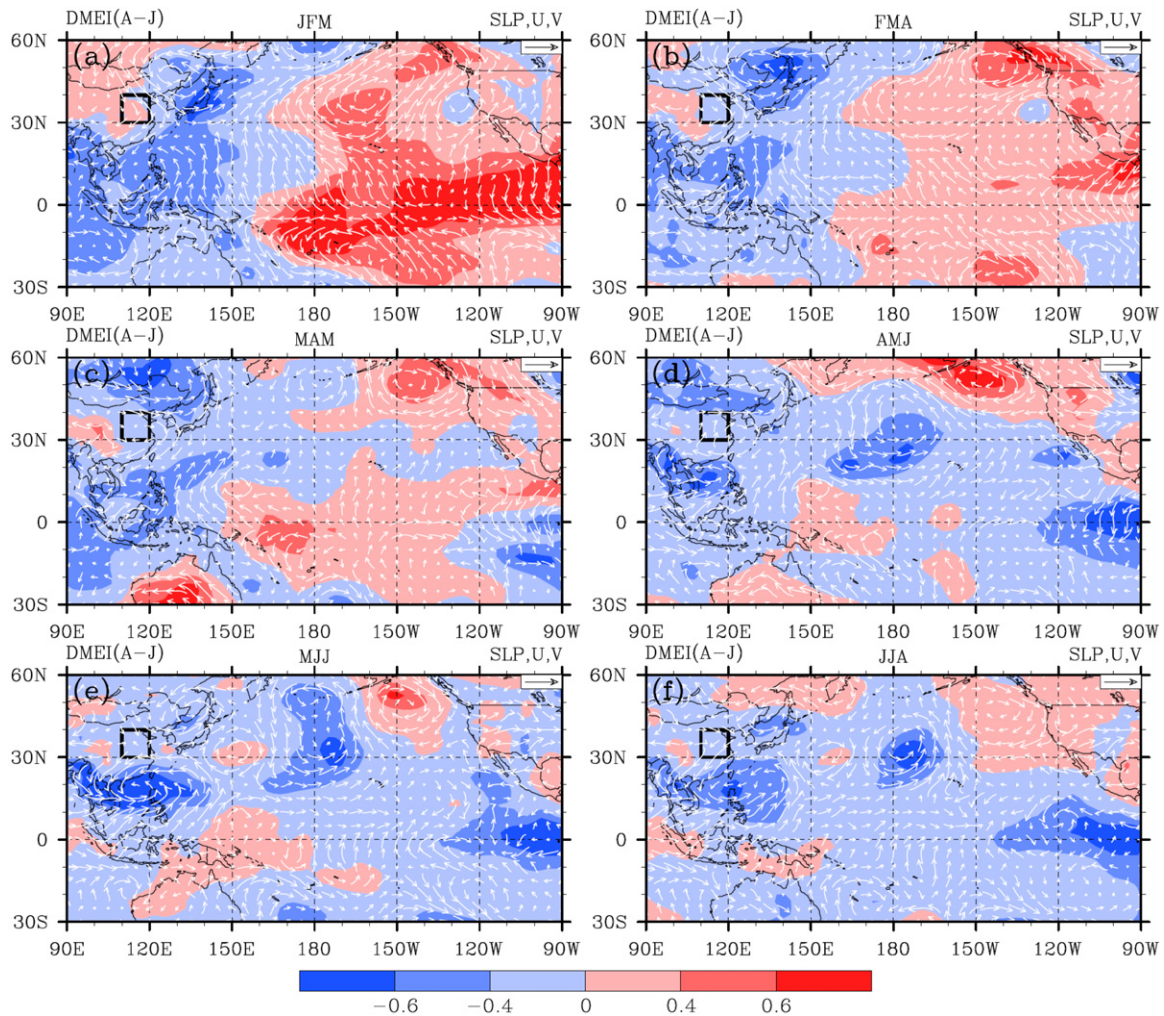
Figure 5. Horizontal distribution of the correlation coefficients between the ΔMEI_{A-J} index and the three-month averaged sea level pressure (SLP, colors) and the 850 hPa wind field (U, V, vectors) at each reanalysis grid in (a) January–February–March (JFM), (b) February–March–April (FMA), (c) March–April–May (MAM), (d) April–May–June (AMJ), (e) May–June–July (MJJ) and (f) June–July–August (JJA) during 2000–2011. The rectangle region is NCP.

captured by emission inventories), could play a significant role in controlling the oscillation of SAOD$_{NCP}$ (Wang *et al* 2012, Liu *et al* 2010, Xu *et al* 2006). Strictly establishing the relationship between emission change and AOD variability is beyond the scope of this study, and will be investigated in future works.

This study reveals that the intra-decadal variability of SAOD$_{NCP}$ could be modulated by ENSO activities even with the possible influence from emission fluctuation. Understanding the relationship between SAOD$_{NCP}$ and ENSO has significant policy inferences. A practical application is to empirically estimate the summertime air quality and visibility over one of the world most populated regions based on the development of winter–spring El Niño activities. When SST over the eastern equatorial Pacific experiences a rapid increase (decrease) in JFMA, the associated weakening (strengthening) of PSAA and enhanced (depressed) easterly over the Yellow Sea ameliorate (degrade) air quality or visibility over NCP in JJA. Therefore, it is of great necessity to consider the influence

of large-scale periodic climate variability when crafting local air quality policies and tracking the subsequent progress.

Besides, the high loading of aerosols over East Asia is shown to account for the surface cooling and precipitation decrease over NCP during the past decades (Zhao *et al* 2006), and thus has a potential to influence regional climate. Climate perturbations in different places are linked through teleconnection. Alternations of El Niño/La Niña episodes set up a large-scale natural forcing (Kim *et al* 2012), which significantly alters the anthropogenic aerosol forcing over EA. Climate response to this forcing perturbation will be further propagated to other places via teleconnection. Therefore, it is important to understand the role of teleconnection in setting up the passage of a regional forcing to a much broader scale, and to explore the circumstances that the superimposed anthropogenic influence would coincide with or trigger extreme weather events.

Finally, the impact of ΔMEI_{A-J} on SAOD is not limited to the NCP. As shown in figure 6, strong correlation between ΔMEI_{A-J} and AOD over the west Africa in DJF,
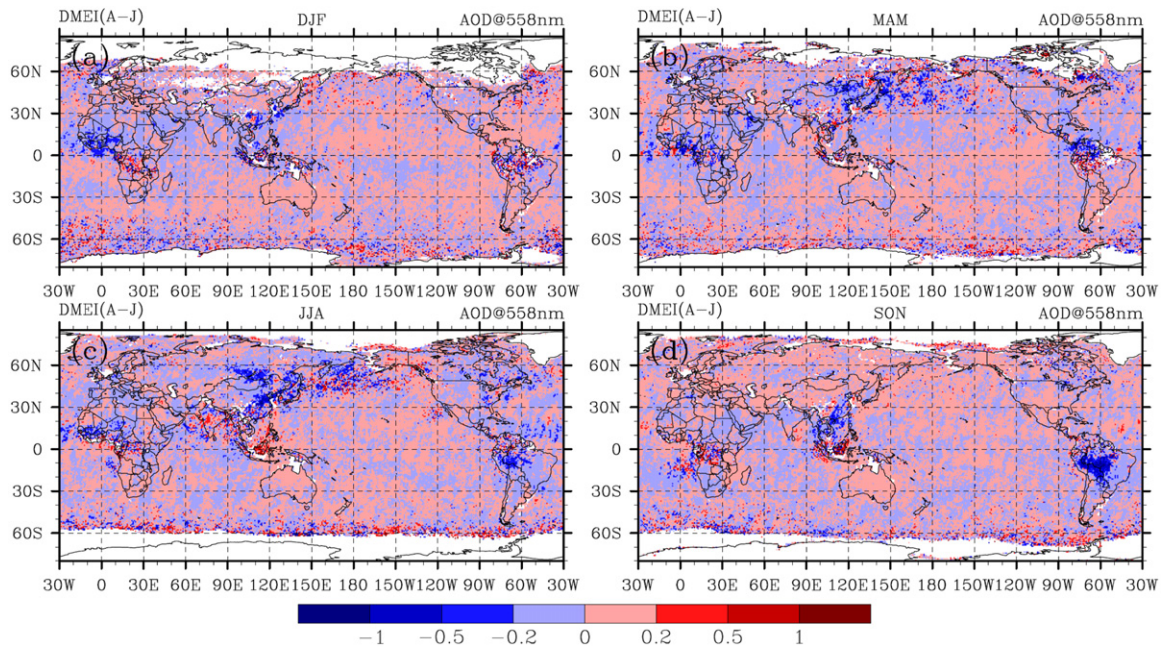
Figure 6. Horizontal distribution of the linear regressions between the ΔMEI_{A-J} index and the seasonal averaged MISR AOD (at 558 nm) at each grid in (a) DJF, (b) MAM, (c) JJA and (d) SON during 2000–2011. The values indicate the change of seasonal AOD due to unit change of the ΔMEI_{A-J} index.

northeastern Asia in MAM and JJA, and the Amazon in SON, implies widespread ENSO-induced forcing of aerosols originating in tropical and boreal forests, and from biomass burning and anthropogenic activities. Signals over the remote oceans may also imply that the ΔMEI_{A-J} index is associated with long-range transport of air pollution (Lang *et al* 2008). Therefore, future studies on chemistry–climate interactions, long-range aircraft measurements as well as emission inventory development referenced on AOD may consider this El Niño effect.

Acknowledgments

References

Adler R F *et al* 2003 The version-2 global precipitation climatology project (GPCP) monthly precipitation analysis (1979-present) *J. Hydrometeorol.* **4** 1147–67

Augustine J A, Hodges G B, Dutton E G, Michalsky J J and Cornwall C R 2008 An aerosol optical depth climatology for NOAA's national surface radiation budget network (SURFRAD) *J. Geophys. Res.-Atmos.* **113** D11204

Barnston A G, Chelliah M and Goldenberg S B 1997 Documentation of a highly ENSO-related SST region in the equatorial Pacific *Atmos. Ocean* **35** 367–83

Deng X J, Tie X X, Zhou X J, Wo D, Zhong L J, Tan H B, Li F, Huang X Y, Bi X Y and Deng T 2008 Effects of Southeast Asia biomass burning on aerosols and ozone concentrations over the Pearl River Delta (PRD) region *Atmos. Environ.* **42** 8493–501

Denman K L *et al* 2007 Couplings between changes in the climate system and biogeochemistry *Climate Change 2007: The Physical Science Basis. Contribution of Working Group I to the Fourth Assessment Report of the Intergovernmental Panel on Climate Change* ed S Solomon, D Qin, M Manning, Z Chen, M Marquis, K B Averyt, M Tignor and H L Miller (Cambridge: Cambridge University Press)

Diner D J *et al* 1998 Multi-angle imaging spectroradiometer (MISR)—instrument description and experiment overview *IEEE Trans. Geosci. Remote* **36** 1072–87

Feng S and Hu Q 2004 Variations in the teleconnection of ENSO and summer rainfall in northern China: a role of the Indian summer monsoon *J. Clim.* **17** 4871–81

Fu T M *et al* 2012 Carbonaceous aerosols in China: top-down constraints on primary sources and estimation of secondary contribution *Atmos. Chem. Phys.* **12** 2725–46

He C, Liu J, Carlton A G, Fan S, Horowitz L W, Levy H and Tao S 2013 Evaluation of factors controlling global secondary organic aerosol production from cloud processes *Atmos. Chem. Phys.* **13** 1913–26

Heald C L, Ridley D A, Kreidenweis S M and Drury E E 2010 Satellite observations cap the atmospheric organic aerosol budget *Geophys. Res. Lett.* **37** L24808

Hsu N C, Gautam R, Sayer A M, Bettenhausen C, Li C, Jeong M J, Tsay S C and Holben B N 2012 Global and regional trends of aerosol optical depth over land and ocean using SeaWiFS measurements from 1997 to 2010 *Atmos. Chem. Phys.* **12** 8037–53

Jacob D J and Winner D A 2009 Effect of climate change on air quality *Atmos. Environ.* **43** 51–63

Janssen N A H *et al* 2011 Black carbon as an additional indicator of the adverse health effects of airborne particles compared with PM10 and PM2.5 *Environ. Health Perspect.* **119** 1691–9

Kaufman Y J, Tanre D and Boucher O 2002 A satellite view of aerosols in the climate system *Nature* **419** 215–23

Kim J S, Kim K Y and Yeh S W 2012 Statistical evidence for the natural variation of the central Pacific El Niño *J. Geophys. Res.-Oceans* **117** C06014

Koch D *et al* 2011 Coupled aerosol-chemistry-climate twentieth-century transient model investigation: trends in short-lived species and climate responses *J. Clim.* **24** 2693–714

Lamarque J F *et al* 2010 Historical (1850–2000) gridded anthropogenic and biomass burning emissions of reactive gases and aerosols: methodology and application *Atmos. Chem. Phys.* **10** 7017–39

Lang C, Tao S, Liu W X, Zhang Y X and Simonich S 2008 Atmospheric transport and outflow of polycyclic aromatic hydrocarbons from China *Environ. Sci. Technol.* **42** 5196–201

Langridge J M *et al* 2012 Evolution of aerosol properties impacting visibility and direct climate forcing in an ammonia-rich urban environment *J. Geophys. Res.-Atmos.* **117** D00v11

Lau N C and Nath M J 2006 ENSO modulation of the interannual and intraseasonal variability of the East Asian monsoon—a model study *J. Clim.* **19** 4508–30

Li B G, Yuan H S, Feng N and Tao S 2010 Spatial and temporal variations of aerosol optical depth in China during the period from 2003 to 2006 *Int. J. Remote Sens.* **31** 1801–17

Lin J, Nielsen C P, Zhao Y, Lei Y, Liu Y and Mcelroy M B 2010 Recent changes in particulate air pollution over China observed from space and the ground: effectiveness of emission control *Environ. Sci. Technol.* **44** 7771–6

Liu J F, Horowitz L W, Fan S M, Carlton A G and Levy H 2012 Global in-cloud production of secondary organic aerosols: implementation of a detailed chemical mechanism in the GFDL atmospheric model AM3 *J. Geophys. Res.-Atmos.* **117** D15303

Liu J F, Mauzerall D L and Horowitz L W 2009a Evaluating inter-continental transport of fine aerosols: (2) global health impact *Atmos. Environ.* **43** 4339–47

Liu J F, Mauzerall D L, Horowitz L W, Ginoux P and Fiore A M 2009b Evaluating inter-continental transport of fine aerosols: (1) methodology, global aerosol distribution and optical depth *Atmos. Environ.* **43** 4327–38

Liu Y, Chen D, Kahn R A and He K B 2009c Review of the applications of multiangle imaging spectroradiometer to air quality research *Sci. China* D **52** 132–44

Liu J *et al* 2010 Validation of multi-angle imaging spectroradiometer aerosol products in China *Tellus* B **62** 117–24

Lu Z, Zhang Q and Streets D G 2011 Sulfur dioxide and primary carbonaceous aerosol emissions in China and India 1996–2010 *Atmos. Chem. Phys.* **11** 9839–64

Mahowald N, Ward D S, Kloster S, Flanner M G, Heald C L, Heavens N G, Hess P G, Lamarque J F and Chuang P Y 2011 Aerosol impacts on climate and biogeochemistry *Annu. Rev. Environ. Resour.* **36** 45–74

Ming Y, Ramaswamy V, Donner L J, Phillips V T J, Klein S A, Ginoux P A and Horowitz L W 2007 Modeling the interactions between aerosols and liquid water clouds with a self-consistent cloud scheme in a general circulation model *J. Atmos. Sci.* **64** 1189–209

Park R J, Jacob D J, Chin M and Martin R V 2003 Sources of carbonaceous aerosols over the United States and implications for natural visibility *J. Geophys. Res.-Atmos.* **108** 4355

Peters A *et al* 2009 Consumption of green vegetables, GSTM1 genotype and the association of air pollution with inflammatory responses *Epidemiology* **20** S160

Pope C A, Burnett R T, Thun M J, Calle E E, Krewski D, Ito K and Thurston G D 2002 Lung cancer, cardiopulmonary mortality, and long-term exposure to fine particulate air pollution *J. Am. Med. Assoc.* **287** 1132–41

Prenni A J, Petters M D, Kreidenweis S M, Heald C L, Martin S T, Artaxo P, Garland R M, Wollny A G and Poschl U 2009 Relative roles of biogenic emissions and Saharan dust as ice nuclei in the Amazon basin *Nature Geosci.* **2** 401–4

Ramanathan V, Crutzen P J, Kiehl J T and Rosenfeld D 2001 Atmosphere—aerosols, climate, and the hydrological cycle *Science* **294** 2119–24

Reddy M S, Boucher O, Bellouin N, Schulz M, Balkanski Y, Dufresne J L and Pham M 2005 Estimates of global multicomponent aerosol optical depth and direct radiative perturbation in the Laboratoire de Meteorologie Dynamique general circulation model *J. Geophys. Res.-Atmos.* **110** D10s16

Smith S J, van Aardenne J, Klimont Z, Andres R J, Volke A and Arias S D 2011 Anthropogenic sulfur dioxide emissions: 1850–2005 *Atmos. Chem. Phys.* **11** 1101–16

Tao M H, Chen L F, Su L and Tao J H 2012 Satellite observation of regional haze pollution over the North China Plain *J. Geophys. Res.-Atmos.* **117** D12203

Wang B, Huang F, Wu Z W, Yang J, Fu X H and Kikuchi K 2009 Multi-scale climate variability of the South China Sea monsoon: a review *Dyn. Atmos. Oceans* **47** 15–37

Wang R *et al* 2012 Black carbon emissions in China from 1949 to 2050 *Environ. Sci. Technol.* **46** 7595–603

Wolter K and Timlin M S 2011 El Nino/Southern Oscillation behaviour since 1871 as diagnosed in an extended multivariate ENSO index (MEI.ext) *Int. J. Climatol.* **31** 1074–87

Xu S S, Liu W X and Tao S 2006 Emission of polycyclic aromatic hydrocarbons in China *Environ. Sci. Technol.* **40** 702–8

Xue F and Liu C Z 2008 The influence of moderate ENSO on summer rainfall in eastern China and its comparison with strong ENSO *Chin. Sci. Bull.* **53** 791–800

Zhao C S, Tie X X and Lin Y P 2006 A possible positive feedback of reduction of precipitation and increase in aerosols over eastern central China *Geophys. Res. Lett.* **33** L11814

Zhu J L, Liao H and Li J P 2012 Increases in aerosol concentrations over eastern China due to the decadal-scale weakening of the East Asian summer monsoon *Geophys. Res. Lett.* **39** L09809